Supporting Information

Polk et al. 10.1073/pnas.1121274109

SI Materials and Methods

Spiking Model. The spiking model used in our study is based on the model presented in the work by Machens et al. (1). The spiking networks consisted of two populations, each with $N = 500$ neurons. Neurons were coupled with inhibitory synaptic connections if they belonged to different populations, whereas there were no connections between neurons that were members of the same population.

The membrane potential of neuron i in population $X \in \{A, B\}$, V_{iX}, obeyed (Eq. **S1**)

$$C\dot{V}_{iX} = g_X^E(V^E - V_{iX}) + g^L(V^L - V_{Xi}) + g_X^I(t)(V^I - V_{iX}) + \sigma\left(\sqrt{c}\xi_{cX}(t) + \sqrt{1-c}\xi_{iX}(t)\right), \quad [S1]$$

(Eq. **S2**)

$$g_X^I(t) = \sum_j wS_{jY}(t) \quad (Y \neq X), \quad [S2]$$

and (Eq. **S3**)

$$\tau_{syn}\dot{S}_{jY} = -S_{jY}. \quad [S3]$$

When a neuron reached its threshold V_{th}, it emitted a spike and was reset to V_{re}. When neuron j in population Y fired, s_j^Y was incremented by $(s_{max} - s_j^Y(t))/s_{max}$, with $s_{max} = 7$. The external fluctuating terms $\xi_{cX}(t)$ and $\xi_{iX}(t)$ were independent Gaussian white noise processes with statistics $\langle\xi(t)\rangle_t = 0$ and $\langle\xi(t)\xi(t')\rangle_t = \delta(t-t')$, where $\langle\cdot\rangle_t$ is an expectation over time. Every neuron received a source of private fluctuations, $\xi_{iX}(t)$, independent from all other stochastic processes and a source of common fluctuation, $\xi_{cX}(t)$. In the local correlations model, the common fluctuations given to population A were independent from the common fluctuations given to population B (i.e., $\langle\xi_{cA}(t)\xi_{cB}(t')\rangle_t = 0$). In the global correlations model, the common fluctuations given to populations A and B were identical (i.e., $\xi_{cA}(t) = \xi_{cB}(t)$). In both cases, $c = 0.05$. For the uncorrelated model, $c = 0$ (Fig. 1).

Values of parameters used in the simulation are reported below.

Parameter	Value
C	0.2 nF
V_{th}	−55 mV
V_{re}	−61 mV
V^E	−5 mV
V^I	−75 mV
τ_{syn}	80 ms
w	0.00116
σ	$\frac{0.12\,\text{mV}}{\sqrt{10}}$

Simulations were performed using Euler–Maruyama integration with a time step of 0.1 ms with custom-made Matlab (Mex) codes.

To control the response of the network during different periods of the trial, the conductances g_A^E, g_B^E were modulated according to the value of the stimuli s. For the loading phase ($s = s_1$), the conductances were (Eq. **S4**)

$$g_X^E = 2.22 + 0.035\,s_1\ \text{nS} \quad [S4]$$

and (Eq. **S5**)

$$g_Y^E = 2.24 - 0.035\,s_1\ \text{nS}. \quad [S5]$$

For the maintenance phase (Eq. **S6**),

$$g_X^E = 2\,\text{nS} \quad [S6]$$

and (Eq. **S7**)

$$g_Y^E = 2\,\text{nS}. \quad [S7]$$

For the decision phase ($s = s_2$) (Eq. **S8**),

$$g_E^X = 2.16 - .035\,s_2\ \text{nS} \quad [S8]$$

and (Eq. **S9**)

$$g_E^Y = 2.14 + .035\,s_2\ \text{nS}. \quad [S9]$$

Population Spike Train Statistics. Let $y_{iX}(t) = \sum_k \delta(t - t_{iX}^k)$ be the spike train of neuron i in population X, with $t_{iX}^k, k = 1, 2, 3\ldots$ as the sequence of spikes produced by the neuron. Population firing rates were computed over a time windows of duration $(t-T, t)$ (Eq. **S10**):

$$r_{iX}(t) = \frac{1}{NT}\int_{t-T}^{t}\sum_{i=1}^{N} y_i^X(t')dt'. \quad [S10]$$

Variance and covariance of the population firing rates were computed as (Eq. **S11**)

$$\text{Var}_X = \left\langle r_X(t)^2\right\rangle_m - \langle r_X(t)\rangle_m^2 \quad [S11]$$

and (Eq. **S12**)

$$\text{Cov}_{AB} = \langle r_A(t) r_B(t)\rangle_m - \langle r_A(t)\rangle_m\langle r_B(t)\rangle_m. \quad [S12]$$

Here, $\langle\cdot\rangle_m$ denotes an expectation across different trials indexed by m; 10,000 trials were used to compute statistics for Figs. 1 and 2, whereas 5,000 trials were used for Fig. 4*F*. Throughout the paper, the population measures used a window length of $T = 10$ ms.

The pairwise statistics (Fig. 2*E*) were computed by first computing the spike count n_{iX} (Eq. **S13**):

$$n_{iX}(t) = \frac{1}{T}\int_{t-T}^{t} y_i^X(t')dt'. \quad [S13]$$

The spike count correlation between neuron i of population X and j or population Y and $\text{Corr}_{(iX\,jY)}$ is computed as (Eq. **S14**)

$$\text{Var}_{(iX)} = \left\langle n_{iX}^2\right\rangle_{m,t} - \langle n_{iX}\rangle_{m,t}^2, \quad [S14]$$

and (Eq. **S15**)

$$\text{Cov}_{(iX\,jY)} = \left\langle n_{iX} n_{jY}\right\rangle_{m,t} - \langle n_{iX}\rangle_{m,t}\left\langle n_{jY}\right\rangle_{m,t}, \quad [S15]$$

and (Eq. **S16**)

$$\mathrm{Corr}_{(iX\,jY)} = \frac{\mathrm{Cov}_{(iX\,jY)}}{\sqrt{\mathrm{Var}_{(iX)}\mathrm{Var}_{(jY)}}}. \quad \textbf{[S16]}$$

Here, $\langle\cdot\rangle_{m,t}$ denotes an expectation across trials (m) and time (t). For the pairwise statistics, $T = 100$ ms.

Random Walk Firing Rate Model. Our phenomenological model for the firing rate activity of a pair of mutually coupled neural populations (Fig. S2*A*) is (Eq. **S17**)

$$\tau\dot{r}_A = -r_A + f(g_\alpha r_B + \mu) + \sigma\left(\sqrt{c}\xi_c(t) + \sqrt{1-c}\xi_A(t)\right) \quad \textbf{[S17]}$$

and (Eq. **S18**)

$$\tau\dot{r}_B = -r_A + f(g_\alpha r_B + \mu) + \sigma\left(\sqrt{c}\xi_c(t) + \sqrt{1-c}\xi_B(t)\right), \quad \textbf{[S18]}$$

where $r_A(t)$ and $r_B(t)$ are the firing rates for populations A and B, respectively. The static input μ is the bias (symmetric across populations) that drives each population during the persistent state period. The constant $g_\alpha < 0$ is the inhibitory coupling between populations, and τ is the effective timescale of population activity. Finally, $\xi_A(t)$ and $\xi_B(t)$ are independent Gaussian white noise processes, whereas $\xi_c(t)$ is another Gaussian white noise process that is shared between the two populations [in all cases, $\langle\xi(t)\rangle_t = 0$ and $\langle\xi(t)\xi(t')\rangle_t = \delta(t-t')$].

The neural transfer $f(x)$ (Fig. S2*B*) is monotonically rising in x and has a nonlinear shape previously proposed (2), because it accurately mimics the dependence of the mean firing rate response of a spiking neuron on a static input x (Eq. **S19**):

$$f(x) = \frac{x}{\hat{\tau}_r x + \tau(1 - e^{-\hat{\beta}x})}, \quad \textbf{[S19]}$$

(Eq. **S20**)

$$\hat{\tau}_r = \frac{\tau_r}{\alpha}, \quad \textbf{[S20]}$$

(Eq. **S21**)

$$\hat{\beta} = \alpha\beta, \quad \textbf{[S21]}$$

and (Eq. **S22**)

$$\mu = \frac{\mu_{max}}{(1 - \mu_{max}\hat{\tau}_r)}. \quad \textbf{[S22]}$$

The saturation of f at high x is defined by the absolute refractory period $\hat{\tau}_r$, whereas τ and $\hat{\beta}$ control the shape of f for moderate x. The nonlinearity of f is parameterized by α. The deterministic nullcline structure $r_B = n_A(r_A)$ and $r_B = n_B(r_A)$ of the firing rate model in Eqs. **S17** and **S18** is given by solutions to $r_A = f(g_\alpha r_B + \mu)$ and $r_B = f(g_\alpha r_A + \mu)$ (here, n_A and n_B are the nullclines of the r_A and r_B dynamics, respectively). For every α, there is a value of g_α that produces the optimal line attractor for our nonlinear model (Eqs. **S17** and **S18**), which is defined by minimizing the integrated square difference $\int_0^{r_{A,max}} (n_B(r_A) - n_A(r_A))^2 dr_A$, where $r_{A,max} = f(\mu_{max})$. For $\alpha = 1$, we find $g_1 = -2.190813$ (Fig. S2*D*, dot), producing a reasonable line attractor where nullclines n_A and n_B overlap significantly over a large range of (r_A, r_B) (Fig. S2*C*). The stochastic model produces random drift along the line attractor similar to the firing rate models (three realizations are shown in Fig. S2*C*).

As $\alpha \to \infty$, the transfer function approaches $f(x) = x$, linearizing the rate model. As α grows, the optimal coupling constant g_α monotonically grows, saturating at $g_\infty = -1$ (Fig. S2*D*). This saturation is such that mutual and self-coupling are equal, producing a degeneracy in the firing rate model. The linear firing rate model has a perfect line attractor; nevertheless, its activity mimics the activity of the nonlinear model (Fig. S2 *C* and *E*). The evolution of the variance and covariance of rate activity is quantitatively matched between the linear and nonlinear models (Fig. S2*F*), further justifying the reduction.

Random Walk Linear Firing Rate Model: Analytic Solution. Our firing rate model ($\alpha \to \infty$ and $g_\infty = -1$ in Eqs. **S17** and **S18**) is a two-variable Ornstein–Uhlenbeck process (3) obeying the stochastic differential system (Eq. **S23**):

$$\tau\dot{\mathbf{r}} = F(\mathbf{r}) + \Gamma\xi(t) \quad \textbf{[S23]}$$

with (Eq. **S24**)

$$\mathbf{r} = \begin{pmatrix} r_A \\ r_B \end{pmatrix}, \quad \textbf{[S24]}$$

(Eq. **S25**)

$$F(\mathbf{r}) = \begin{pmatrix} -r_A - r_B + I \\ -r_B - r_A + I \end{pmatrix}, \quad \textbf{[S25]}$$

(Eq. **S26**)

$$\Gamma = \begin{pmatrix} \sqrt{1-c} & 0 & \sqrt{c} \\ 0 & \sqrt{1-c} & \sqrt{c} \end{pmatrix}, \quad \textbf{[S26]}$$

and (Eq. **S27**)

$$\xi(t) = \sigma\begin{pmatrix} \xi_A(t) \\ \xi_B(t) \\ \xi_c(t) \end{pmatrix}. \quad \textbf{[S27]}$$

We first solve for the eigenvalues λ and eigenvectors $\mathbf{u}$ of the deterministic ($\sigma = 0$) system (Eq. **S28**):

$$\lambda^{(1)} = 0, \quad \textbf{[S28]}$$

(Eq. **S29**)

$$\mathbf{u}^{(1)} = \frac{1}{\sqrt{2}}\begin{pmatrix} 1 \\ -1 \end{pmatrix}, \quad \textbf{[S29]}$$

(Eq. **S30**)

$$\lambda^{(2)} = \frac{-2}{\tau}, \quad \textbf{[S30]}$$

and (Eq. **S31**)

$$\mathbf{u}^{(2)} = \frac{1}{\sqrt{2}}\begin{pmatrix} 1 \\ 1 \end{pmatrix}. \quad \textbf{[S31]}$$

We remark that the symmetric neighbor and self-coupling with $g_\infty = -1$ produces a zero eigenvalue $\lambda^{(1)}$, with eigenvector $\mathbf{u}^{(1)}$ being the line attractor for the persistent state (Fig. 3*B*, green line).

The probability density $P(r_A, r_B, t | r_A^0, r_B^0, 0)$ obeys the associated Fokker–Planck (Eq. **S32**) for Eq. **S23**:

$$\frac{\partial P}{\partial t} = \left[\frac{\partial}{\partial r_A}\left(\frac{r_A}{\tau} + \frac{r_B}{\tau}\right) + \frac{\partial}{\partial r_B}\left(\frac{r_A}{\tau} + \frac{r_B}{\tau}\right)\right]P + \frac{\sigma^2}{2\tau^2}\left[\frac{\partial^2}{\partial r_A^2} + \frac{2c\partial^2}{\partial r_A \partial r_B} + \frac{\partial^2}{\partial r_B^2}\right]P \quad \textbf{[S32]}$$

with initial condition (Eq. **S33**)

$$P(r_A, r_B, 0) = \delta(r_A - r_A^0)\delta(r_B - r_B^0). \quad \textbf{[S33]}$$

We note that the diffusion terms in the Fokker–Planck equation satisfy the diffusion matrix D (Eq. **S34**):

$$D = \frac{\sigma^2}{2\tau}\Gamma\Gamma' = \frac{\sigma^2}{2\tau}\begin{pmatrix} 1 & c \\ c & 1 \end{pmatrix}. \quad \textbf{[S34]}$$

A Gaussian form for $P(r_A, r_B, t \mid r_A^0, r_B^0, 0)$ satisfies Eq. **S32** (Eq. **S35**):

$$P(\mathbf{r}, t) = \frac{1}{2\pi\sqrt{|\Sigma(t)|}} \exp\left(-\frac{1}{2}(\mathbf{r}-\boldsymbol{\mu})'\Sigma(t)^{-1}(\mathbf{r}-\boldsymbol{\mu})\right). \quad \textbf{[S35]}$$

To calculate the covariance matrix $\Sigma(t)$, we first derive the Green's function G using the eigenvalues and eigenvectors from Eqs. **S28–S31**. This derivation allows a calculation for the evolution of the density given an initial condition. The entries of G are given by (Eq. **S36**)

$$G_{ij} = \sum_{\alpha=1,2}\left(e^{\lambda^{(\alpha)}t}\mathbf{u}_i^{(\alpha)}\mathbf{u}_j^{(\alpha)}\right) \Rightarrow G = \begin{pmatrix} \frac{1}{2}+\frac{e^{\frac{-2t}{\tau}}}{2} & -\frac{1}{2}+\frac{e^{\frac{-2t}{\tau}}}{2} \\ -\frac{1}{2}+\frac{e^{\frac{-2t}{\tau}}}{2} & \frac{1}{2}+\frac{e^{\frac{-2t}{\tau}}}{2} \end{pmatrix}. \quad \textbf{[S36]}$$

Using G, we find the time-dependent covariance matrix $\Sigma(t)$ entries (Eq. **S37**):

$$\Sigma_{ij}(t) = \sum_s \int_0^t G_{ik}\, G_{js}\, d\hat{\tau}\, 2D_{ks}, \quad \textbf{[S37]}$$

and (Eq. **S38**)

$$\begin{aligned}\Sigma_{11}(t) &= \Sigma_{22}(t) \\ &= \int_0^t G_{11}G_{11}\, d\hat{\tau}\, 2D_{11} + 2\int_0^t G_{11}G_{12}\, d\hat{\tau}\, 2D_{12} \\ &\quad + \int_0^t G_{12}G_{12}\, d\hat{\tau}\, 2D_{22} \\ &= \frac{\sigma^2 t(1-c)}{2\tau^2} + \frac{\sigma^2(1+c)\left(\tau - \tau e^{\frac{-4t}{\tau}}\right)}{8\tau^2}, \end{aligned} \quad \textbf{[S38]}$$

and (Eq. **S39**)

$$\begin{aligned}\Sigma_{12}(t) &= \Sigma_{21}(t) \\ &= 2\int_0^t G_{11}G_{21}\, d\hat{\tau}\, 2D_{11} + \int_0^t G_{11}G_{22}\, d\hat{\tau}\, 2D_{12} \\ &\quad + \int_0^t G_{12}G_{21}\, d\hat{\tau}\, 2D_{21} \\ &= \frac{\sigma^2 t(c-1)}{2\tau^2} + \frac{\sigma^2(c+1)\left(\tau - \tau e^{\frac{-4t}{\tau}}\right)}{8\tau^2}. \end{aligned} \quad \textbf{[S39]}$$

We see that, for large t, the first term dominates, and the variance and covariance behave as (Eq. **S40**)

$$\mathrm{Var}(r_X) = \frac{\sigma^2 t(1-c)}{2\tau^2} \quad \textbf{[S40]}$$

and (Eq. **S41**)

$$\mathrm{Cov}(r_A, r_B) = \frac{\sigma^2 t(c-1)}{2\tau^2}. \quad \textbf{[S41]}$$

To quantitatively compare the reduced model to the spiking simulations, we fit the two reduced model parameters (σ, c) using Eqs. **S40** and **S41**. For the spiking model with local fluctuations, we set $c = 0$, and σ was determined by a linear fit (in time) of $\mathrm{Var}(r_X)(t)$ from Eq. **S40** to the variance results obtained from spiking simulations (Fig. 3*D*). The time constant τ was taken to be 80 ms, corresponding to the synaptic time constant used in the simulations. Then, for the spiking model with global correlations, c was determined by fitting $\mathrm{Cov}(r_A, r_B)(t)$ from Eq. **S41** to the $\mathrm{Cov}(r_A, r_B)(t)$ obtained from spiking simulations (Fig. 3*E*). We set σ to be equal to the value obtained from the local simulations.

Probability of Correct Decision. To compute the probability of a decision, we numerically integrated $P(\mathbf{r}, t)$ from Eq. **S35** over the region determined by the decision boundary (quadrature algorithm). The decision boundary line is given by $r_B = r_A + \Delta$, where the offset Δ is determined such that the line intersects the unstable saddle point that appears during the decision phase (full model in Eqs. **S17** and **S18**).

1. Machens CK, Romo R, Brody CD (2005) Flexible control of mutual inhibition: A neural model of two-interval discrimination. *Science* 307:1121–1124.
2. Abbott LF, Chance FS (2005) Drivers and modulators from push-pull and balanced synaptic input. *Prog Brain Res* 149:147–155.
3. Risken H (1996) *The Fokker–Planck Equation: Methods of Solution and Applications* (Springer, New York), 2nd Ed.

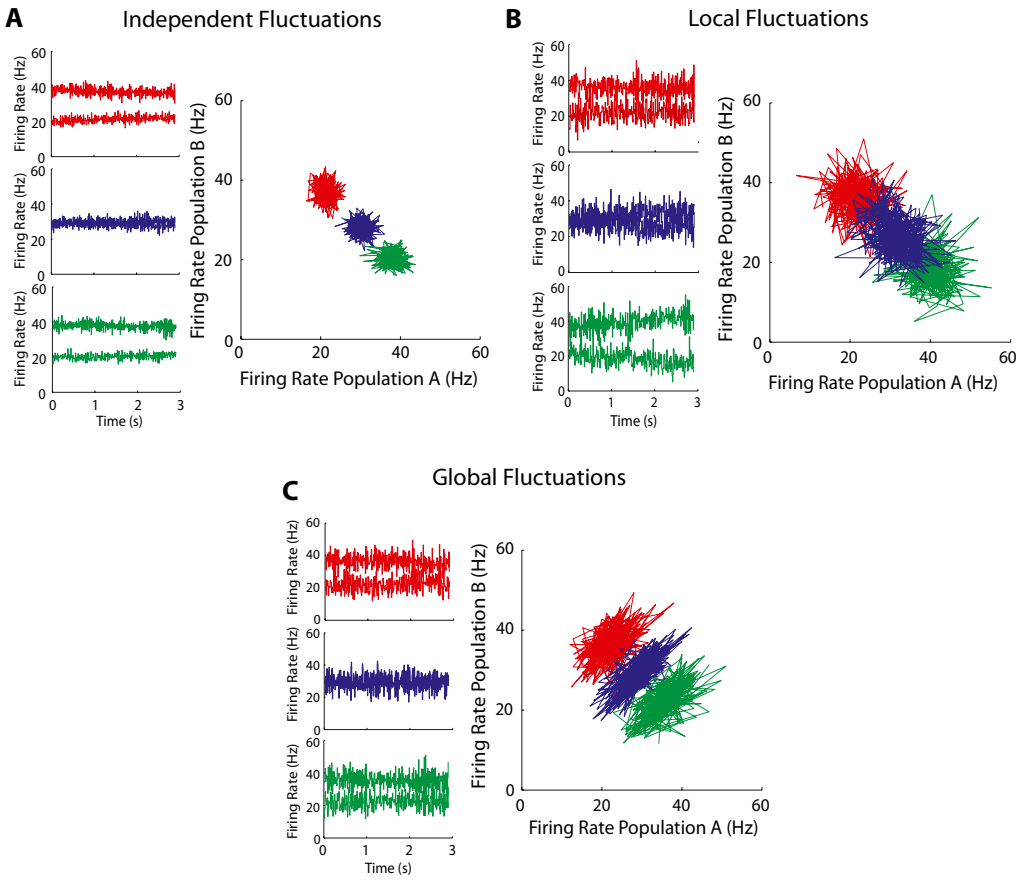

Fig. S1. Stimulus-specific persistent activity for the spiking networks with correlated fluctuations. (*A*) Network with uncorrelated external fluctuations; the time series for three stimulus conditions (*Left*) shows stable persistent activity that is a reflection of the stimulus conditions. The rate activity in (r_A, r_B) space shows a clear separation for all three stimulus conditions. (*B*) Same as *A* but for the network with local correlations. (*C*) Same as *A* but for the network with global correlations. The colors in all panels are as described in Fig. 1.

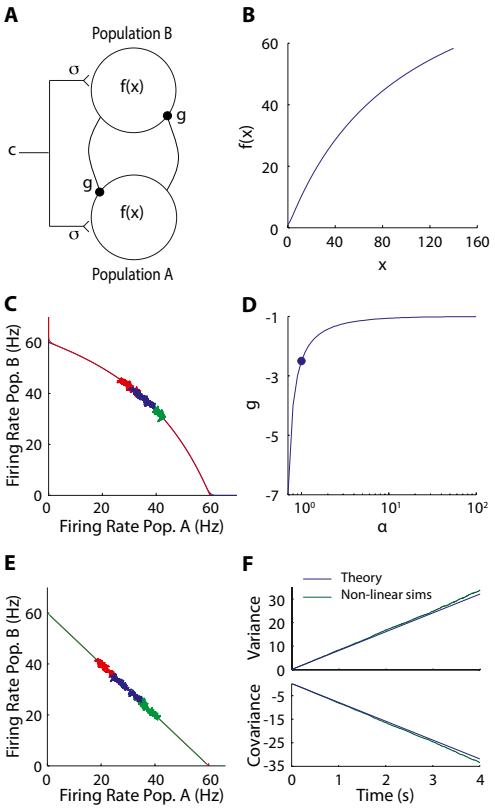

Fig. S2. Nonlinear and linear phenomenological firing rate models. (*A*) Schematic of firing rate model with transfer $f(x)$, fluctuation variance σ^2, and correlation c. (*B*) Transfer function $f(x)$ with $\mu_{max} = 60$, $\tau = 1$, $\tau_r = 0.01$, $\beta = 1$, and $\alpha = 1$. (*C*) Nullclines n_A and n_B (red curves) when $\alpha = 1$ and $g(\alpha) = -2.190813$ chosen to minimize the integral of the square difference between n_A and n_B. Three realizations are shown (colors) with distinct initial conditions. (*D*) The population coupling $g(\alpha)$ that yields the optimal line attractor. As $\alpha \to \infty$, the coupling g tends to -1. (*E*) Linear nullclines n_A and n_B for $\alpha \to \infty$ and $g = -1$. Three realizations are shown (colors) with distinct initial conditions. (*F*) Comparison between trial variance (*Upper*) and covariance (*Lower*) computed from the nonlinear ($\alpha = 1$) and linear models ($\alpha \to 1$).

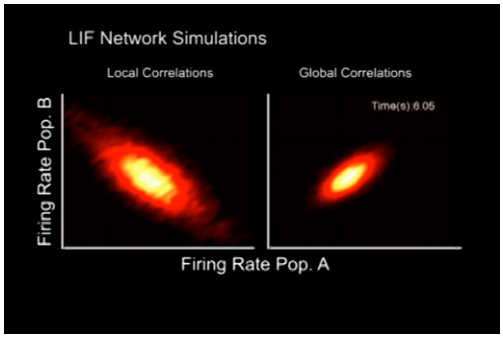

Movie S1. Video showing the evolution of the probability density of population rates $P(r_A, r_B, t)$ for $0 < t < 10$ s estimated from repeated trials of the spiking network model. The local (*Left*) and global (*Right*) correlation schemes are shown. The (r_A, r_B) grid was sampled at 1 Hz, and $P(r_A, r_B, t)$ was smoothed for presentation.

Movie S1

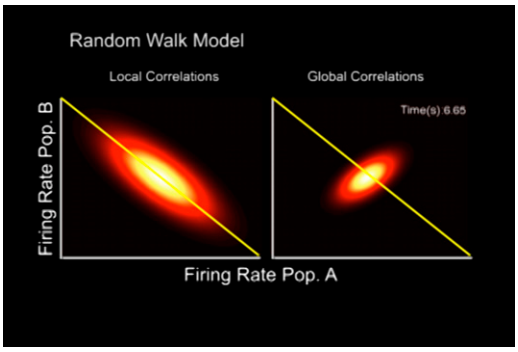

Movie S2. Video showing the evolution of the probability density of population rates $P(r_A, r_B, t)$ for $0 < t < 10$ s computed from the linear, random walk firing rate model. The local (*Left*) and global (*Right*) correlation schemes are shown.

Movie S2